Study of Substrate Energy Dissipation Mechanism in in-Phase and Anti-Phase Micromachined Vibratory Gyroscopes

Alexander A. Trusov, Adam R. Schofield, and Andrei M. Shkel
MicroSystems Laboratory, Department of Mechanical and Aerospace Engineering
University of California, Irvine, Irvine, CA, USA
Email: {atrusov, aschofie, ashkel}@uci.edu

***Abstract*— This paper analyzes energy dissipation mechanisms in in-phase and anti-phase actuated micromachined z-axis vibratory gyroscopes. The type of actuation is experimentally identified as the key factor to energy dissipation. For in-phase devices, dissipation through the die substrate is the dominant energy loss mechanism. This damping mechanism depends strongly on the die attachment method; rigid attachment increases Q-factor at the cost of reduced isolation of the MEMS device from package stresses and vibrations. In contrast, anti-phase operation suppresses dissipation through the die substrate while providing immunity to external vibrations. Higher Q-factors in anti-phase devices are explained by effective subtraction of stresses applied to the substrate during vibrations. Based on the experimental investigation and the developed analytical model for energy dissipation through the die substrate, the limiting Q-factor for in-phase devices is generally below 20 thousand, while Q-factors much higher than 100 thousand can be achieved with balanced anti-phase actuated gyroscopes.**

I. Introduction

Performance limits of various vibratory micromachined devices, including Coriolis gyroscopes, are dictated by the maximum achievable Q-factors of the operational vibratory modes [1], [2]. For gyroscopes packaged at pressures near atmospheric, viscous gas damping dominates the other dissipation mechanisms [3]; extensive literature on gas damping in different types of MEMS is available [4].

Dissipation of energy in micromachined vibratory gyroscopes operated in vacuum is defined by a combination of several mechanisms [2], including thermoelastic dissipation (TED), surface losses, dissipation through support, and electronic damping [5]. Existing publications on dissipation in vacuum operated gyroscopes mainly focus on TED limitations [5], [6].

While thermoelastic dissipation often becomes the Q-factor limiting mechanism in vacuum packaged micromechanical resonators due to their decreasing size and increasing frequency (MHz range) [6], it does not necessarily dominate damping in micromachined gyroscopes which usually have a bulky proof mass and operate in lower frequencies (kHz range). The observed limiting non-viscous Q-factor, Q_{lim}, of most micromachined gyroscopes in vacuum is in the range of 10^3 to 10^4. In contrast, finite element modeling shows that Q-factor due to solely TED is usually higher than 10^6.

The other important non-viscous energy loss mechanism, dissipation of energy through the substrate, is not sufficiently studied, especially in the context of MEMS gyroscopes [2]. Limited literature is available on this dissipation mechanism and mostly studies propagation of vibrational energy of micromachined beams into a much larger substrate, e.g. [7]–[9].

In this paper, we comparatively analyze dissipation of energy through the die substrate in in-phase and anti-phase actuated z-axis micromachined vibratory gyroscopes and study the effects of die attachment method. First, in Section II, we report the measurements of drive-mode Q-factors in gyroscopes with in-phase and an anti-phase actuation packaged using different die attachment methods. Then, in Section III, we propose a lumped element model that considers damped dynamics of a finite die substrate and provides insight into experimentally observed effects of actuation type and die attachment method on the effective Q-factor. Finally, the paper is concluded with a summary of the obtained results and a discussion on the high-Q sensor design and packaging trade-offs in Section IV.

II. Experimental Characterization

A. Testbed Gyroscopes and Experimental Setup

Two different types of gyroscopes were used for experimental study of Q-factors. The first gyroscope [10] has only one degree of freedom (DOF) drive-mode corresponding to a single resonance of the proof mass. The second gyroscope [11] has a 2-DOF drive-mode which allows for two distinct resonances: the lower frequency in-phase mode and the higher frequency anti-phase mode. In the in-phase mode the two proof masses of [11] translate in unison, similarly to the gyroscope with a 1-DOF drive-mode [10]. Because of the similarity between the 2-DOF in-phase mode and the single resonant mode of a 1-DOF device, we will refer to both cases as "in-phase" or "in-phase actuated". Correspondingly, the anti-phase resonance of a 2-DOF drive-mode will be referred to as "anti-phase" or "anti-phase actuated".

The tested gyroscopes were fabricated using an in-house wafer-scale SOI process, singulated, packaged in CDIP-24 packages, and wirebonded for experimental characterization, Fig. 2(a). In order to investigate effect of the die attachment on the measured Q-factor, the gyroscopes were attached to the packages using three different methods: SPI conductive

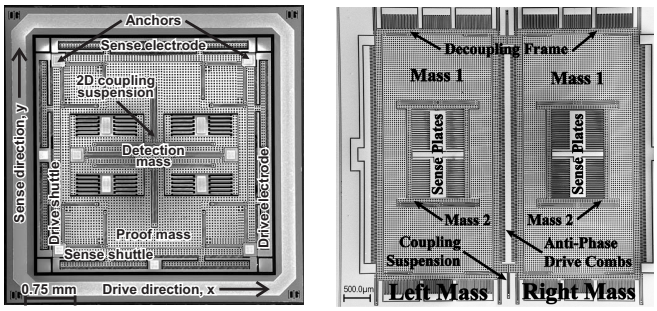

(a) Gyroscope [10] with a 1-DOF drive-mode.

(b) Gyroscope [11] with a 2-DOF drive-mode.

Fig. 1. SEM images of gyroscopes with 1-DOF and 2-DOF drive-modes.

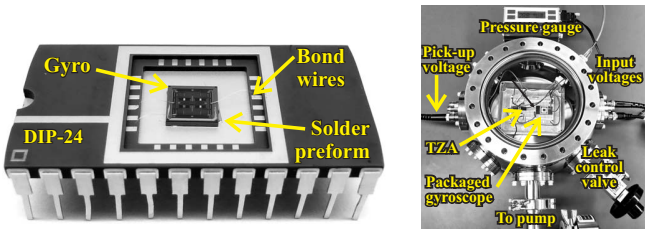

(a) Packaged gyroscope [10].

(b) Vacuum setup.

Fig. 2. Experimental setup for characterization of Q-factors in vacuum.

double-sided carbon adhesive tape, Circuit Works two-part conductive epoxy, and SPM Au-Sn 80/20 solder preform. In order to experimentally measure dependency of the Q-factor on pressure and identify the limiting non-viscous value Q_{lim}, the packaged gyroscopes were characterized in a vacuum chamber, Fig. 2(b).

B. Effects of Actuation Type and Die Attachment

For each tested device, Q-factors were measured at different pressure levels between atmospheric and 10 mTorr vacuum. The measured Q-factors as functions of pressure were then analyzed to separate out the effect of gas damping and extract the limiting non-viscous Q_{lim}. Fig. 3 presents the experimental results for both in-phase and anti-phase actuated gyroscopes packaged using different die attachment methods.

Fig. 3(a) shows Q-factors of the in-phase and anti-phase resonant modes of the gyroscope [11]. The in-phase mode Q_{lim} strongly depends on the die attachment method, with Q_{lim} of approximately 3.6 and 10.6 thousand for adhesive and epoxy die attachment, respectively. At the same time, Q_{lim} of the anti-phase mode is not significantly affected by the die attachment method. In the tested range of vacuum, the dissipation is governed by molecular gas flow damping mechanism and shows Q_{lim} of approximately 200 thousand, more than an order of magnitude higher than for the in-phase mode.

The effect of die attachment on the limiting Q-factor, Q_{lim}, was further investigated using a batch of identical in-phase actuated gyroscopes [10] with a single-DOF drive-mode, Fig. 3(b). These devices were packaged using three different

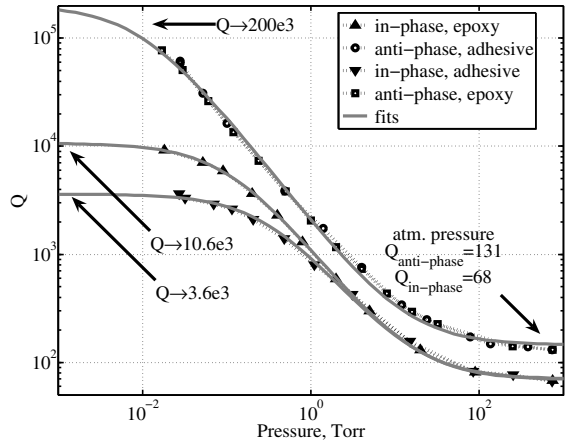

(a) Gyroscope [11] with a 2-DOF drive-mode having both an in-phase and and an anti-phase mode.

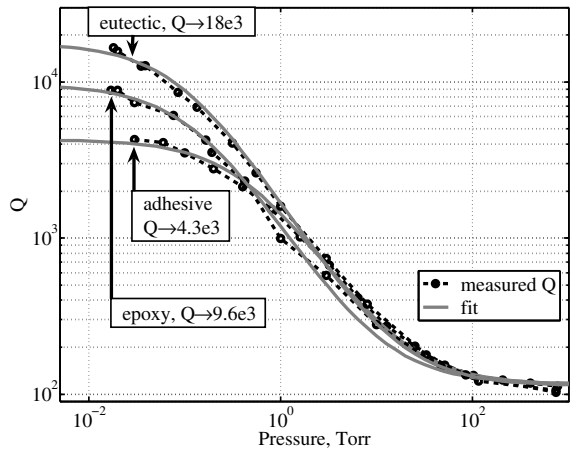

(b) In-phase gyroscope [10] with a single-DOF drive-mode.

Fig. 3. Experimental study of Q-factor in in-phase and anti-phase actuated gyroscopes packaged using different die attachment methods.

die attachment methods: 1) carbon adhesive, 2) epoxy, 3) eutectic solder preform. The measurements reveal an increasing Q_{lim} of approximately 4.3, 9.6, and 18 thousand, respectively.

The experimental results suggest that the limiting energy dissipation mechanism in in-phase actuated devices is dissipation of energy through the die substrate into the package via the die attachment interface with the more rigid and less viscous attachment material resulting in higher Q_{lim}.

III. Modeling

A. Finite Element Modeling of Thermoelastic Dissipation

In this subsection, we report a numerical simulation of thermoelastic dissipation to verify the experimental conclusions on the nature of the dominant Q-factor limiting loss mechanism. The gyroscope [11] with 2-DOF drive-mode was modeled using the finite element software package COMSOL Multiphysics. Finite Element Modeling (FEM) of the gyroscope's in-phase and anti-phase modes is shown in Fig. 4(a) and Fig. 4(b), respectively. For both the in-phase and the anti-phase modes, Q-factor due to thermoelastic damping, Q_{TED},

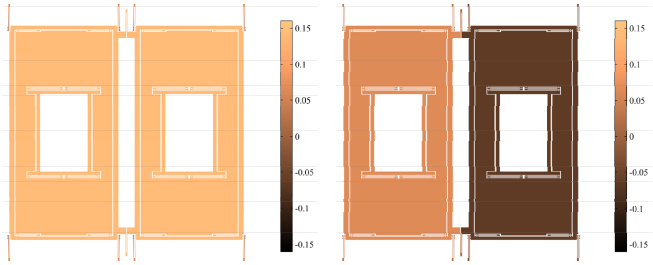

(a) In-phase mode, $Q_{TED} = 1.7 \times 10^6$, resonance is at 1.46 kHz.

(b) Anti-phase mode, $Q_{TED} = 1.3 \times 10^6$, resonance is at 2.18 kHz.

Fig. 4. FEM of TED in gyroscope [11] predicts Q-factors higher than 10^6 for both in-phase and anti-phase modes (colors represent x-displacement).

exceeds a million, which is orders of magnitude higher than the experimentally observed Q_{lim}. These modeling results support the experimental conclusions on importance of energy dissipation through the die substrate as the Q-factor limiting mechanism.

B. Dissipation in In-Phase Actuated Devices

It is apparent from the reported experiments and finite element modeling that dissipation of energy through the vibrating die substrate via the die attachment interface can be the dominant energy dissipation mechanism. Thus, the dynamics of the die substrate needs to be considered together with the dynamics of a MEMS gyroscope's drive-mode. Fig. 5(a) shows a lumped model of a single-DOF vibratory element m_1 on a mobile die substrate m_2. The ratio between the device and the die substrate masses depends mostly on the relative thicknesses of the layers and the relative area of the device; for the in-phase actuated SOI devices discussed in this paper $m_2 \approx 20 \times m_1$. The interaction between the vibratory element m_1 and the die substrate m_2 is described by stiffness k_1 and damping c_1; die attachment interface between the die substrate m_2 and the fixed package is represented by k_2 and c_2.

According to this approach, an ideal single mass MEMS resonator, such as a 1-DOF drive-mode of a vibratory gyroscope, is in fact a coupled dynamic system with 2 degrees of freedom, where the observed characteristics of the main resonant mode are affected by the coupling from the die substrate dynamics. Fig. 5(b) illustrates the concept by comparing the nominal 1-DOF and the coupled frequency responses of a single-DOF resonator with intrinsic Q-factor of 200 thousand on a mobile die substrate. For this simulation, the following numerical parameters, based on the identified properties of the test devices, were used: m_1 = 7.3e-7 kg, m_2 = 1.4e-5 kg, k_1 = 115 N/m, k_2 = 9e3 N/m, and c_1 = 4.6e-8 N/(m/s). The damping value c_2 associated with the energy loss at the die attachment interface was defined by $c_2 = \sqrt{k_2 m_2}/Q_{sub}$, where the quality factor of the die attachment Q_{sub} was iterated through 10^1, 10^2, 10^3, and 10^4. Due to the die substrate coupling, the observed Q-factor of the MEMS device can drop drastically. For instance, for $Q_{sub} = 10$ [12] the simulation shows that effective Q-factor can drop from 200 thousand to below a

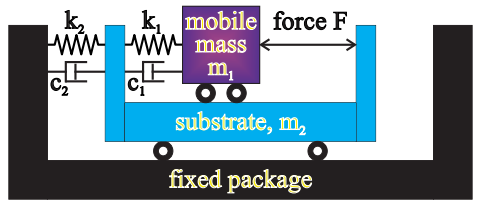

(a) Lumped model augmented with the die substrate DOF.

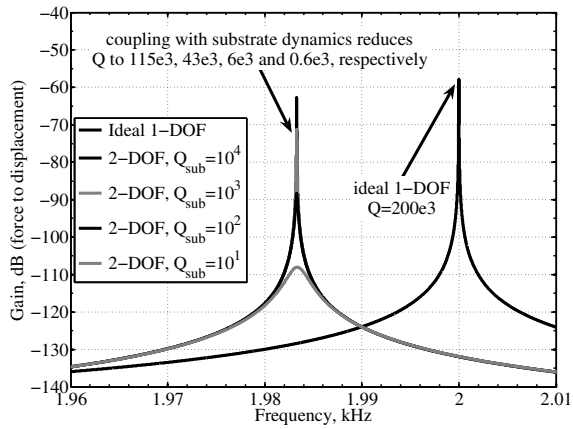

(b) Nominal and die substrate coupled frequency responses for different die attachment damping values.

Fig. 5. Modeling of energy loss through the substrate by coupling a high-Q gyroscope with a mobile die substrate with damped die attachment interface.

thousand. Values of Q_{sub} on the order of several hundred result in effective Q-factors observed in the experiments.

C. Dissipation in Anti-Phase Actuated Devices

Similarly to the case of a drive-mode with a single degree of freedom discussed in the previous subsection, dissipation of energy through the substrate in devices with 2-DOF, such as drive-mode of tuning fork gyroscopes, can be modeled by augmenting the lumped model with an extra DOF representing the mobile die substrate. Fig. 6(a) shows a lumped model, where m_1 and m_2 are the two tines of a tuning fork type gyroscope, and m_3 is the mobile die substrate. Each tine is suspended relative to the substrate with stiffnesses $k_{1,2}$ and damping $c_{1,2}$ respectively; the two tines are also coupled together with stiffness k_{12} and damping c_{12}. The die attachment interface between the mobile die substrate m_3 and the fixed package is represented by stiffness k_3 and damping c_3.

Typically, the two tines of a tuning fork gyroscope are designed to be structurally balanced, i.e. $m_1 = m_2$, $k_1 = k_2$, and $c_1 = c_2$. For the SOI anti-phase actuated gyroscopes described in this paper, $m_3 \approx 120 \times m_{1,2}$. Fig. 6(b) shows simulation of the substrate dissipation using the lumped 3-DOF model. In the simulation, the frequency response of a balanced tuning fork gyroscope with an anti-phase mode Q-factor of 200 thousand is compared to the response of the 3-DOF system that includes the damped die substrate dynamics. The following numerical parameters, based on the properties of the gyroscopes with a 2-DOF drive-mode implemented in a

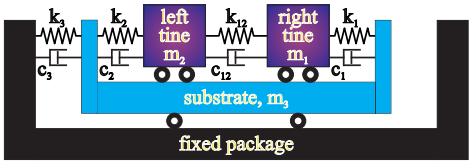

(a) Lumped model: the two tines $m_{1,2}$ and the mobile die substrate m_3 on the fixed package.

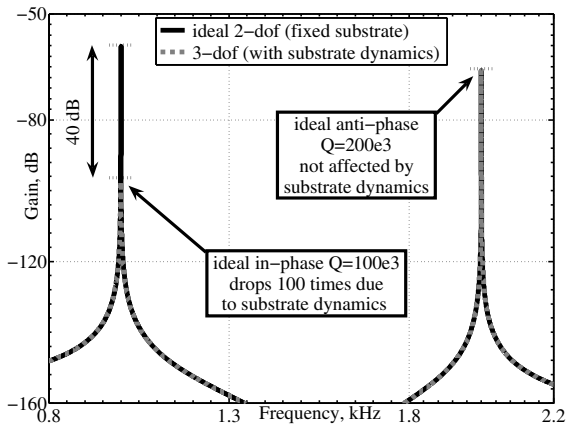

(b) High-Q frequency response and effect of die substrate damping.

Fig. 6. Modeling of energy loss through the substrate in 2-DOF devices by augmenting the system dynamics with a damped die substrate DOF.

3.5 mm die size, were used for the simulation: $m_{1,2}$ = 1.16e-7 kg, m_3 = 1.4e-5 kg, $c_{1,2}$ = 7.3e-9 N/(m/s), $k_{1,2}$ = 4.6 N/m, k_{12} = 7 N/m, k_3 = 9e3 N/m, and $c_3 \approx 1$ N/(m/s). Similarly to the experimental results in Section II, the modeled frequency responses illustrate that the effective Q-factor of the in-phase mode can drastically drop due to dynamic coupling with the damped die substrate. The anti-phase mode Q-factor of a balanced tuning-fork is robust to the die substrate damping.

IV. Conclusions

We presented a study of Q-factor limitations in micromachined z-axis vibratory gyroscopes. The type of actuation was identified as the key factor to the dominant energy dissipation mechanism and the maximal achievable Q_{lim}.

For in-phase actuated devices, energy dissipation through the die substrate is the dominant damping mechanism. Rigid die attachment, such as eutectic bonding, minimizes the substrate dissipation and allows for Q_{lim} on the order of 10 thousand. In practice, however, compliant die attachments are often used to reduce vibrational and stress isolation of the MEMS device from the package [13], which results in a several-fold reduction of Q_{lim}.

Well balanced anti-phase operation suppresses dissipation through the substrate due to effective cancelation of stresses applied by the mobile structures to the die substrate, achieving Q-factors much higher than 100 thousand. The high Q-factor of anti-phase operational modes does not depend on the die attachment properties, allowing for compliant die attachment in order to minimize the mechanical stress coupling between the package and the sensing element [13]. In addition, anti-phase driven gyroscopes inherently provide mechanical rejection of common mode vibrations [11].

Acknowledgment

This work was supported by the National Science Foundation Grant CMS-0409923, Custom Sensors & Technologies Systron Donner Automotive (CS&T SDA, formerly BEI Technologies) contract BEI-36974, and UC Discovery program ELE04-10202. The tested gyroscopes were fabricated at the UC Irvine Integrated Nanosystems Research Facility (INRF). Design of the gyroscopes and experimental characterization were performed at the UC Irvine MicroSystems Laboratory. The authors would like to acknowledge David Virissimo of Semiconductor Packaging Materials (SPM) for the help with eutectic attachment process development, and Cenk Acar and Lynn E. Costlow of CS&T SDA for stimulating discussions.

References

[1] X. Liu, J. F. Vignola, H. J. Simpson, B. R. Lemon, B. H. Houston, and D. M. Photiadis, "A loss mechanism study of a very high Q silicon micromechanical oscillator," *Journal of Applied Physics*, vol. 97, no. 2, p. 023524, 2005.

[2] Z. Hao, M. F. Zaman, A. Sharma, and F. Ayazi, "Energy loss mechanisms in a bulk-micromachined tuning fork gyroscope," in *Proc. IEEE Sensors Conference*, 2006, pp. 1333–1336.

[3] J. A. Geen, S. J. Sherman, J. F. Chang, and S. R. Lewis, "Single-chip surface micromachined integrated gyroscope with 50 deg/h Allan deviation," *J. Solid-State Circuits*, vol. 37, no. 12, pp. 1860–1866, 2002.

[4] M. Bao and H. Yang, "Squeeze film air damping in MEMS," *Sensors and Actuators, A: Physical*, vol. 136, no. 1, pp. 3–27, 2007.

[5] A. Duwel, J. Gorman, M. Weinstein, J. Borenstein, and P. Ward, "Experimental study of thermoelastic damping in MEMS gyros," *Sensors and Actuators A: Physical*, vol. 103, no. 1-2, pp. 70–75, Jan. 2003.

[6] R. N. Candler, H. Li, M. Lutz, W.-T. Park, A. Partridge, G. Yama, and T. W. Kenny, "Investigation of energy loss mechanisms in micromechanical resonators," in *Proc. International Solid-State Sensors, Actuators and Microsystems Conference TRANSDUCERS 2003*, vol. 1, 2003, pp. 332–335.

[7] Z. Hao, A. Erbil, and F. Ayazi, "An analytical model for support loss in micromachined beam resonators with in-plane flexural vibrations," *Sensors and Actuators, A: Physical*, vol. 109, no. 1-2, pp. 156–164, 2003.

[8] Y.-H. Park and K. C. Park, "High-fidelity modeling of MEMS resonators – part I: anchor loss mechanisms through substrate," *J. Microelectromechanical Systems*, vol. 13, no. 2, pp. 238–247, 2004.

[9] ——, "High-fidelity modeling of MEMS resonators – part II: coupled beam-substrate dynamics and validation," *J. Microelectromechanical Systems*, vol. 13, no. 2, pp. 248–257, 2004.

[10] A. A. Trusov, A. R. Schofield, and A. M. Shkel, "New architectural design of a temperature robust MEMS gyroscope with improved gain-bandwidth characteristics," in *Proc. A Solid-State Sensors, Actuators and Microsystems Workshop (Hilton Head Workshop 2008)*, 2008, pp. 14–17.

[11] A. R. Schofield, A. A. Trusov, and A. M. Shkel, "Multi-degree of freedom tuning fork gyroscope demonstrating shock rejection," in *Proc. IEEE Sensors Conference*, 2007, pp. 120–123.

[12] B. Le Foulgoc, T. Bourouina, O. Le Traon, A. Bosseboeuf, F. Marty, C. Breluzeau, J.-P. Grandchamp, and S. Masson, "Highly decoupled single-crystal silicon resonators: an approach for the intrinsic quality factor," *J. Micromechanics and Microengineering*, vol. 16, no. 6, pp. 45–53, 2006.

[13] U.-M. Gomez, B. Kuhlmann, J. Classen, W. Bauer, C. Lang, M. Veith, E. Esch, J. Frey, F. Grabmaier, K. Offterdinger, T. Raab, H.-J. Faisst, R. Willig, and R. Neul, "New surface micromachined angular rate sensor for vehicle stabilizing systems in automotive applications," in *Proc. International Solid-State Sensors, Actuators and Microsystems Conference TRANSDUCERS 2005*, vol. 1, 2005, pp. 184–187 Vol. 1.